JOURNAL OF AIRCRAFT
Vol. 41, No. 3, May–June 2004

Limit-Cycle Oscillations of Aircraft Caused by Flutter-Induced Drag

Mayuresh J. Patil*
Virginia Polytechnic Institute and State University, Blacksburg, Virginia 24061

It has been shown in earlier work that the energy for flutter comes from propulsion, that is, flutter leads to an increase in drag. The present paper seeks to explain the effect of flutter-induced drag on aircraft response. It is shown that the aircraft can undergo limit-cycle oscillations even if the oscillations are in the linear structural and aerodynamic lift range. These limit-cycle oscillations occur as a result of the inability of the engine to support exponentially increasing oscillations. The limit-cycle oscillations are composed of variations in flight speed and amplitude of vibration. This modality of limit-cycle oscillations has not been presented in earlier literature and leads to better understanding of the limit-cycle oscillation problem.

Introduction

LIMIT-CYCLE oscillations (LCOs) of wings and aircraft is an important problem that has received a lot of attention over the last few decades. LCO is normally associated with nonlinearities in the system. Nonlinearities in the structure or the aerodynamic forces can induce preflutter LCO or lead to limiting of the amplitude of oscillations of an unstable system (postflutter LCO). Various researchers have done experimental and theoretical investigation of the effect of aerodynamic and structural nonlinearities on the LCOs in wings and airfoil.[1–4] This paper examines the postflutter LCO behavior in flexible aircraft, which does not originate from structural or aerodynamic lift nonlinearity.

Flutter is not a usual operating condition. In fact, flutter is avoided even in flight-test environment. Still understanding postflutter behavior is important from a scientific perspective and would be necessary for any controlled, postflutter operation in the future. Also, military aircraft encounter LCO, which shrinks the operational envelope of the aircraft. In the past, LCO studies have been restricted to nonlinearities stemming from structure or aerodynamics. The effect of flutter-induced drag on LCOs has not been considered. As a first step toward understanding the effect of flutter-induced drag, the postflutter response of an otherwise linear system is studied here.

Energy Considerations

The limit-cycle oscillations presented in this paper can be understood based on the energy-transfer mechanisms responsible for aeroelastic response. Earlier work by the author[5] shows that there exist three types of modes in an aeroelastic system: 1) unstable, drag-producing mode (flutter mode), 2) stable, drag-producing mode, and 3) stable, thrust-producing mode (flapping-flight mode).

Figure 1 illustrates the energy-transfer characteristics of each type of mode during constant amplitude oscillations at constant flight speed. Energy produced, energy lost, and/or work done as a result of structural vibration, aerodynamic wake, and propulsion are taken into account. The figure shows three energy sinks/sources: 1) structure; which denotes the energy of the structure, the direction of energy flow indicating the work done by or on the structure; 2) wake, which denotes the energy lost in the fluid; and 3) propulsion, which denotes the work done by the engine to maintain a given flight speed. If the structural energy is increasing, it indicates an unstable (flutter) mode, whereas decreasing structural energy indicates a damped mode, that is, external work has to be done on the structure to maintain a level of oscillations. Wake energy is the kinetic energy of the fluid caused by the vorticity shed in an otherwise stationary flow. This energy is constantly increasing. Finally, flow of energy from propulsion indicates a requirement of higher thrust to maintain a constant flight speed and thus denotes a drag-producing mode. Flow of energy into propulsion indicates that the mode produces thrust. This propulsive energy is in addition to that required to maintain the trim condition.

For the flutter mode it is observed that the energy is pumped into the structure. Because the energy is also lost in the wake, the energy required to support the structural instability must come from the propulsion. Thus, as the system goes into flutter additional propulsive energy is required to maintain the flight speed, that is, additional thrust is required to counteract the increase in the drag of the airplane.

Flutter and Drag

It is clear that when the wing flutters the energy to sustain this growing motion comes from propulsion, that is, when the wing starts to oscillate in the flutter mode it leads to increase in the drag. Thus, to maintain the aircraft speed the engine needs to increase the thrust. This is the increase in energy expenditure that results in flutter and increase in structural (and wake) energy. This phenomenon is not obvious if the flight speed is assumed constant while solving aeroelastic problems as is usually done. With the assumption of constant flight speed, it is implicit that whatever thrust required to maintain that flight speed is provided by the engine.

For the present study, it is assumed that the thrust is not increased to maintain the flutter speed, but rather a specified thrust is applied (as required for steady trimmed flight). Thus, as the system starts to flutter the drag on the aircraft will increase, and the aircraft will decelerate. One can only speculate at this point on the dynamic system response, but it can be seen that the problem is now coupled between the flight speed and the oscillation amplitude. The flight speed determines the stability of the wing and thus the rate of change of oscillation amplitude of the wing (whether it will decay or grow exponentially). On the other hand, the amplitude of oscillation determines the drag on the aircraft and thus the rate of change of flight speed of the aircraft (whether it will accelerate or decelerate).

One possible solution is if the aircraft goes down to the critical flutter speed and oscillates at an amplitude, which leads to loss of energy in aerodynamic wake equal to the excess of propulsive energy. This type of LCO seems to be the only possible steady periodic solution. Another solution involves a periodic change in the flight speed and the amplitude of vibration. A chaotic variation in the flight speed and oscillation amplitude is also possible.

Presented as Paper 2002-1409 at the AIAA/SDM 43rd, Denver, CO, 22–25 April 2002; received 31 March 2002; revision received 6 August 2003; accepted for publication 6 October 2003. Copyright © 2003 by Mayuresh J. Patil. Published by the American Institute of Aeronautics and Astronautics, Inc., with permission. Copies of this paper may be made for personal or internal use, on condition that the copier pay the $10.00 per-copy fee to the Copyright Clearance Center, Inc., 222 Rosewood Drive, Danvers, MA 01923; include the code 0021-8669/04 $10.00 in correspondence with the CCC.

*Assistant Professor, Department of Aerospace and Ocean Engineering. Member AIAA.

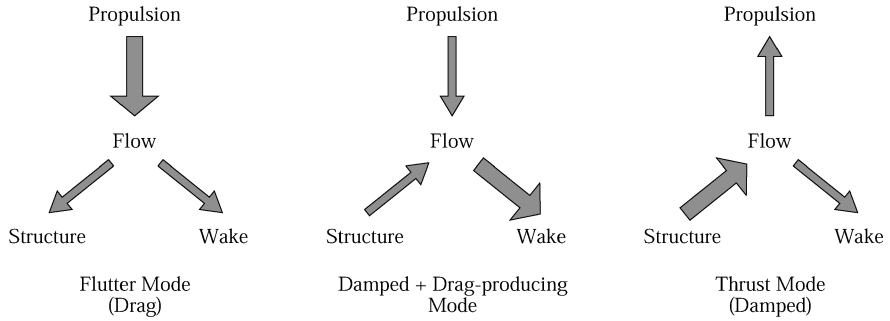

Fig. 1 Energy transfer pathways in aeroelasticity.

The objectives of this work are to develop an analysis that takes into account the increase in induced drag at flutter and determine its effect on the flight dynamics of the aircraft. Such a study will provide insight into the energetics of flutter and the dynamics of LCO.

Analysis Methodology

The analysis methodology is based on a simple beam model for the structure and the fixed-wake, unsteady vortex lattice method[6] for aerodynamics. The wing is modeled using the mode shapes in bending and torsion for a cantilevered beam. In the unsteady vortex lattice method, vortices (of unknown vortex strengths) are distributed on the wing as well as in the wake. Three conditions are then imposed on the vortex strengths to solve the problem. These conditions are summarized next.

Vorticity-downwash relation relates the downwash on the wing caused by structural deflections to the downwash induced by bound and wake vorticity

$$K_b\Gamma_b^{n+\frac{1}{2}} + K_w\Gamma_w^{n+\frac{1}{2}} - W^{n+\frac{1}{2}} = 0 \tag{1}$$

where Γ_b and Γ_w denote the strengths of bound and wake vortices, K_b and K_w are the corresponding induced velocity coefficients, W denotes the downwash caused by structural deflections, and the superscript denotes the time iteration at which the variable is calculated. Superscript $n+\frac{1}{2}$ denotes the imposition of the vorticity-downwash constraint at a time between iteration n and iteration $n+1$.

Shed vorticity-bound vorticity relation relates the change in bound vorticity to the wake vorticity shed in that time interval:

$$\Sigma\Gamma_b^n - \Sigma\Gamma_b^{n+1} - \Gamma_{w_1}^{n+1} = 0 \tag{2}$$

where $\Sigma\Gamma_b$ denotes the summation of the bound vorticity over a given airfoil section and Γ_{w_i} denotes the ith wake vortex at the section.

Convection of shed vorticity relation states that at each iteration the vorticity travel at the freestream flight speed to the next vortex element:

$$\Gamma_{w_{i+1}}^{n+1} - \Gamma_{w_i}^n = 0 \tag{3}$$

The preceding equations form a complete set of equations representing the dynamics of bound and wake vorticity. The set of equations represents a discrete-time linear system. After a discrete-time to continuous-time transformation, the continuous-time wake dynamic equations can be written as

$$\{\dot{\Gamma}\} = [A_1]\{\Gamma\} + [A_2]\{W\} \tag{4}$$

where $[A_1]$ and $[A_2]$ are coefficient matrices that relate the vorticity $\Gamma = \{\Gamma_b, \Gamma_w\}^T$ to structural deformations W. W can be written in terms of the structural displacement variables.

The aerodynamic equations are coupled with the structural equations to form a complete aeroelastic set. The structural equations as derived using the beam mode shapes are given by

$$[M]\{\ddot{q}\} + [K]\{q\} = \{Q\} \tag{5}$$

where $[M]$ and $[K]$ are the mass and stiffness matrices, $\{q\}$ are the modal displacement, and $\{Q\}$ are the modal forces.

The modal forces are calculated from the aerodynamic lift distribution. The lift distribution is given by

$$L = \rho U\Gamma_b + \rho\int_{-b}^{x}\dot{\Gamma}_b\,\mathrm{d}x \tag{6}$$

where ρ is the air density and U is the flight speed.

Equations (4) and (5) form a set of linear aeroelastic equations that predict the linear response and stability of a wing in an airflow.

As described earlier, flutter will induce drag, and, consequently, the flight speed will change. The equation for the dynamics of the aircraft is given by

$$M_{\text{aircraft}}\dot{U} = T - \tfrac{1}{2}\rho U^2 S C_{D0} - D_{\text{induced}} \tag{7}$$

where M_{aircraft} is the mass of the aircraft, T is the thrust, C_{D0} is the viscous drag coefficient, and D_{induced} is the induced drag. The equation only takes into account the dynamics of the aircraft in terms of flight-speed changes. The rigid-body dynamics of the aircraft in pitch and plunge are neglected as the present focus is on the effects on the flight speed. For a linear aeroelastic system as analyzed here, the addition of aircraft pitch-and-plunge degrees of freedom will lead to change in the flutter speed and mode shape. The magnitude of the change will depend on the interaction between the aeroelastic and flight dynamic modes. Here it is assumed that this interaction is negligible.

Induced drag is a quadratic term, but, in the absence of a linear drag term, it is quite important even for small motions. The induced drag has a steady component because of the trailing vortices and an unsteady component because of the shed wake vortices. The induced drag can be expressed as[7]

$$D_{\text{induced}} = \rho w_z\Gamma_b + \rho\alpha\int_{-b}^{x}\dot{\Gamma}_b\,\mathrm{d}x \tag{8}$$

where w_z is the downwash at the vortex location caused by trailing and wake vortices and α is the geometrical angle of attack.

Equations (4), (5), and (7) together form a complete set of aeroelastic equations for the dynamics of the complete aircraft.

Results

Results are presented for an aircraft with high-aspect-ratio wing. The geometric and structural data for the aircraft are given in Table 1. The structure is modeled using five bending and five torsion modes. The airflow is modeled using 50 wing (bound) vortices and 125 wake (shed) vortices distributed over 5 spanwise and 25 chordwise stations (over five chord lengths).

Table 1 Model data

Parameter	Value
Wing	
Half-span	16 m
Chord	1 m
Mass per unit length	0.75 kg/m
Mom. inertia (50% chord)	0.1 kg m
Spanwise elastic axis	50% chord
Center of gravity	50% chord
Bending rigidity	2×10^4 N m^2
Torsional rigidity	1×10^4 N m^2
Bending rigidity (in-plane)	5×10^6 N m^2
Fuselage	
Mass of fuselage	48 kg
Viscous drag coefficient	0.1
Flight condition	
Altitude	20 km
Density of air	0.0889 kg/m^3

Two-Dimensional Comparisons

Before studying the aeroelastic characteristics of a wing, it is essential to gauge the accuracy of the unsteady vortex lattice method (UVLM) in predicting the aerodynamic forces, especially the drag. Because exact solutions are not available for the three-dimensional problem, a two-dimensional UVLM time-marching solution is checked against two-dimensional Theodorsen results.

For a two-dimensional airfoil oscillating in pitch and plunge, the expressions for the lift L and drag D can be written as[5]

$$L = 2\pi\rho b\left[b/2(U\dot{\alpha} + \ddot{h}) + C(k)U\left(U\alpha + \dot{h} + \tfrac{1}{2}b\dot{\alpha}\right)\right]$$

$$D = L\alpha - 2\pi\rho b\left[C(k)\left(U\alpha + \dot{h} + \tfrac{1}{2}b\dot{\alpha}\right) - \tfrac{1}{2}b\dot{\alpha}\right]^2 \qquad (9)$$

where h and α are the midchord plunge and pitch angle; ρ, b, U are the air density, semichord, airspeed, respectively; and $C(k)$ is the Theodorsen's function that depends on the reduced frequency $k = \omega b/U$. The preceding expressions are frequency-domain solutions for harmonic structural deformations.

The lift and drag given by Theodorsen/Garrick (TG) are now compared with the results of the two-dimensional time-domain unsteady vortex lattice method. Figure 2 shows the aerodynamic response to harmonic input as calculated by the UVLM. The lift and drag from the UVLM calculations should approach the TG results after a few oscillations. Figure 2a shows the normalized lift response to a sinusoidal plunge input. As can be seen in the figure, the lift predicted by the UVLM is almost the same as that predicted by TG. Figure 2b shows the corresponding drag. Again, the UVLM results match the TG results. Also, as expected, the drag data show that 1) average drag is not zero; 2) drag varies with a frequency twice that of the motion; 3) for pure plunging motion, drag is negative (i.e., there is thrust). Figures 2c and 2d show the lift and drag for pitch oscillations. Again, the comparison with TG is excellent. This shows that the UVLM can capture the unsteady flowfield quite accurately and, consequently, leads to accurate prediction of the aerodynamic forces.

Three-Dimensional Lift and Drag

Figure 3 shows the aerodynamic response for a three-dimensional wing. Here the wing is oscillated in either the first bending or the first torsion mode. The amplitude of oscillations is such that the tip displacement is 1 m for the bending mode while the tip twist is 0.1 radians for the torsion mode. Figure 3a shows the total unsteady lift acting on the wing oscillating in the first bending mode. A reduced frequency of 0.25 and a flight speed of 35 m/s are used for the calculations. Figure 3b shows the corresponding induced drag on the wing. Again, as expected, bending oscillations produce thrust. Finite wings produce trailing vortices, which produce drag, and thus thrust generated by finite wings is less than that by a corresponding two-dimensional airfoil. It is seen that, unlike the two-dimensional case, the thrust is negative (induced drag is positive) over a small portion of the oscillation.

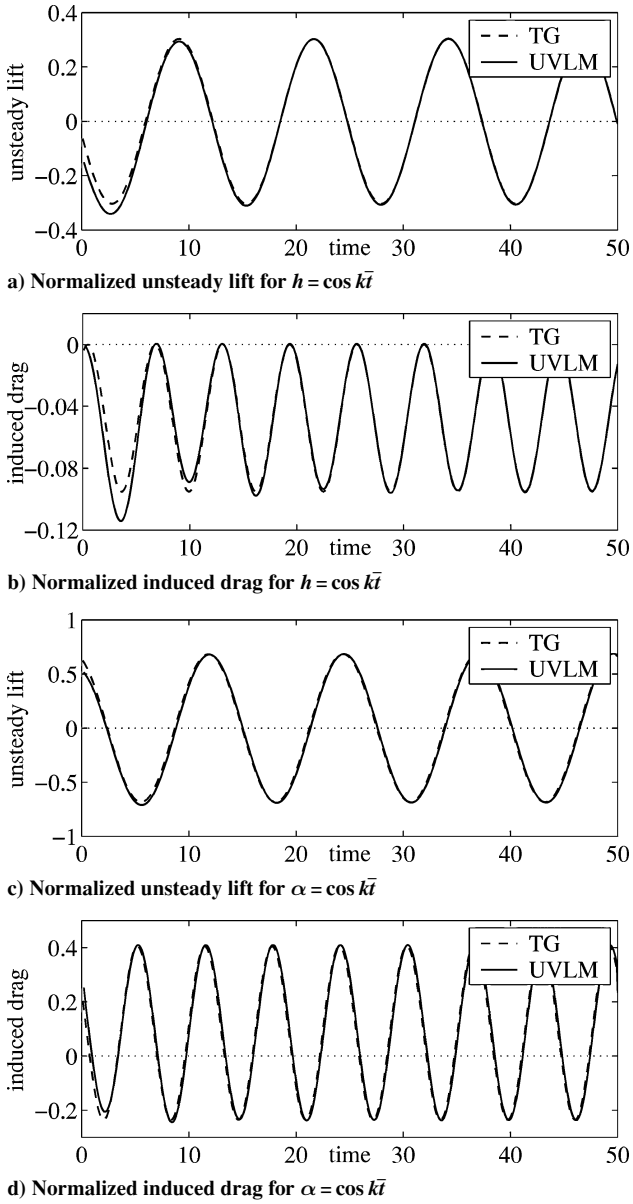

Fig. 2 Comparison of normalized unsteady lift and induced drag for two-dimensional airfoil at $k = 0.5$.

The magnitude of the thrust is of the same order as the magnitude of the lift even for not-so-large oscillation (1-m tip displacement on a 16-m wing). It should be reiterated that the drag is a quadratic function of the oscillation amplitude while the lift is linearly related to the oscillation amplitude. Thus, the drag will increase at a higher rate with increase in amplitude as compared to lift. The results underscore the importance of induced drag forces in aeroelastic analysis, especially for large-amplitude oscillations.

Figures 3c and 3d show the lift and drag for oscillations in the first torsion mode. Again, a reduced frequency of 0.25 and a flight speed of 35 m/s are used for the calculations. Here one sees that the first torsion mode produces drag and not thrust.

Postflutter Response

The aeroelastic model described in the earlier section is now used to calculate the aeroelastic response of the wing and aircraft. The flutter calculations give the flutter speed for the wing to be 33.4 m/s. A wing flying at speeds above the flutter speed is analyzed. Linear stability theory predicts that any disturbances to the wing will grow exponentially and will continue to infinity for a linear system.

Figure 4 shows the tip displacement, tip twist, and the flight speed for a wing at a trim condition of 35 m/s. A disturbance of 0.01 radians tip twist in the first torsion mode is provided to the system. If the

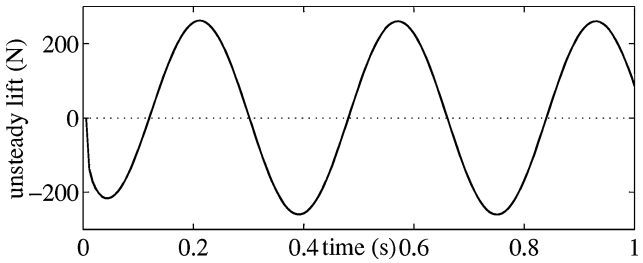

a) Unsteady lift for $h_{\text{bend}_1} = \cos \omega t$

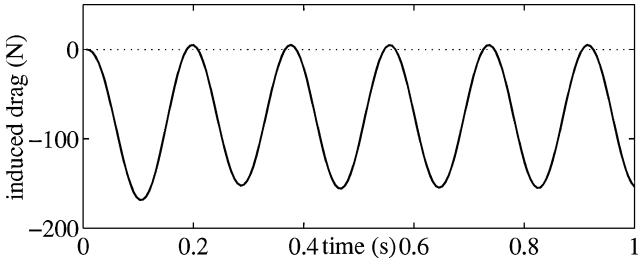

b) Induced drag for $h_{\text{bend}_1} = \cos \omega t$

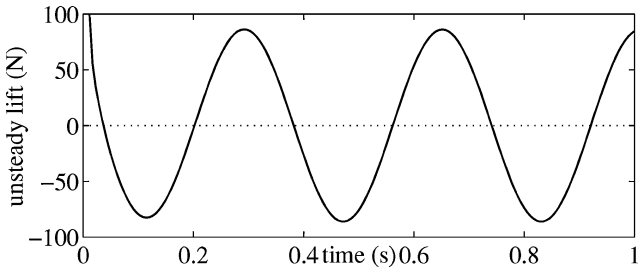

c) Unsteady lift for $\alpha_{\text{tors}_1} = 0.1 \cos \omega t$

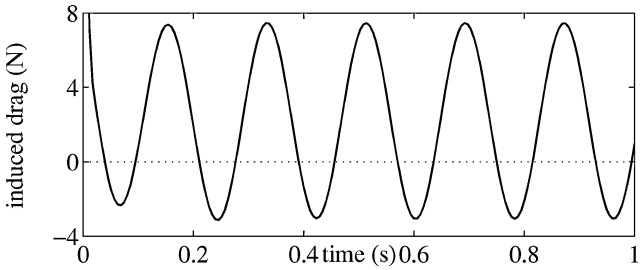

d) Induced drag for $\alpha_{\text{tors}_1} = 0.1 \cos \omega t$

Fig. 3 Unsteady lift and drag for the wing at $k = 0.25$ and $U = 35$ m/s.

wing is assumed to maintain the trim flight speed of 35 m/s, it is seen that the response (tip displacement and tip twist) increases exponentially, exceeding practical limits within 10 s. One can analyze the role of structural and aerodynamic nonlinearities in restricting the amplitude of oscillations. Analysis of such LCOs has been presented earlier[4] and is not the focus of the present work.

Figure 4 also presents the response of the aircraft as a whole to the same initial flight speed and disturbance. Flight speed is allowed to vary as given by Eq. (7). Now, as the wing oscillation amplitude increases exponentially there is a corresponding increase in the drag on the wing. This leads to a decrease in the flight speed. As the flight speed decreases, it falls below the flutter speed, and the wing oscillation amplitude starts to decrease exponentially. Thus, as shown in the figure, taking into account the aircraft dynamics, it is clear that the oscillation amplitude does not increase indefinitely.

LCO

When the aircraft is trimmed at a flight speed above flutter, the wing starts to oscillate, the drag increases, and thus the flight speed decreases. Essentially, the wing oscillation amplitude as well as the flight speed change with time. Figure 5 shows the aircraft response (tip displacement, tip twist, and flight speed) over a longer duration

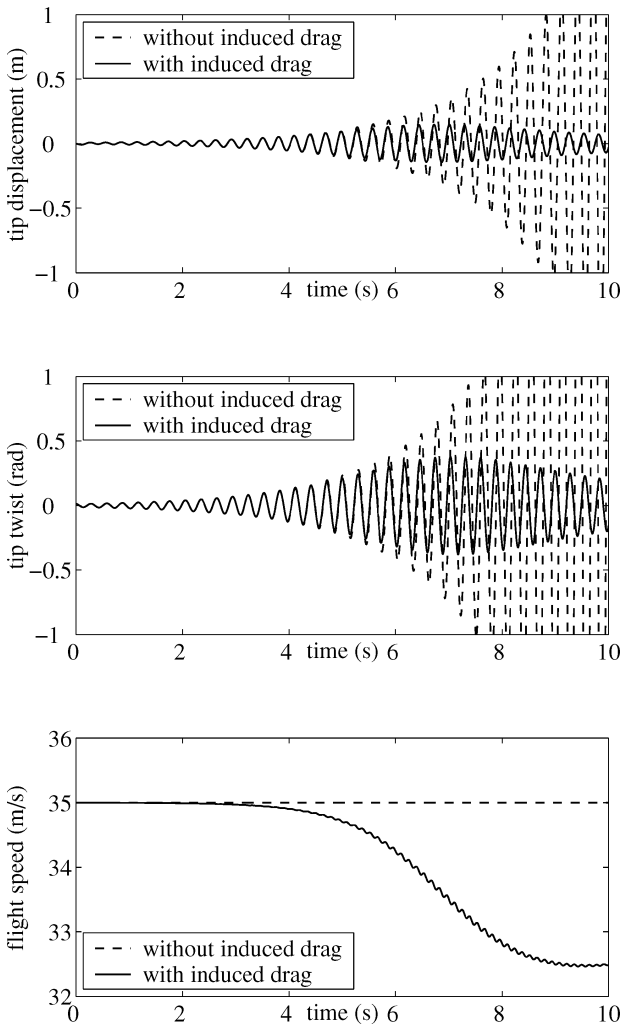

Fig. 4 Comparison of postflutter response with and without induced drag effects at $U = 35$ m/s.

(100 s). The flight-speed subfigure shows that the aircraft speed oscillates about the flutter speed. The tip displacement and tip twist subfigures show that the amplitude of (bending-twist) vibration also oscillates. This is expected because, as the flight speed decreases below flutter speed, the oscillation amplitude starts to decrease, and as the oscillation amplitude decreases so does the drag. The aircraft then accelerates to a speed above flutter speed leading to an increase in the amplitude of vibration, and the process repeats itself. There are two frequencies and amplitudes to be noted. First one has to deal with the frequency and amplitude of the bending-twist aeroelastic vibrations. The other has to do with the frequency and amplitude of the oscillation of the amplitude of bending-twist vibration as well as the flight speed oscillations. The first frequency is dependent on the flexible wing modes, whereas the second frequency is dependent on the flight dynamic equation. The aeroelastic mode frequency is much higher than the flight dynamic frequency.

Figure 5 shows that the oscillations in the flight speed decrease and the flight speed approaches the flutter speed. There is a corresponding decrease in the oscillation of the vibration amplitude, and it approaches a constant amplitude oscillation. Thus, the aircraft trimmed at a flight speed above the flutter speed approaches the flutter speed if the thrust is held constant. At the flutter speed, the flutter mode is neutrally stable, and a constant amplitude vibration is maintained. The amplitude of vibration is such that the effective drag is equal to the difference between the thrust provided for the trim flight and the thrust necessary for the flight at the flutter speed. Thus, the drag induced by flutter leads to a LCO such that the structure vibrates with constant amplitude in the flutter mode and the flight speed is maintained at the flutter speed.

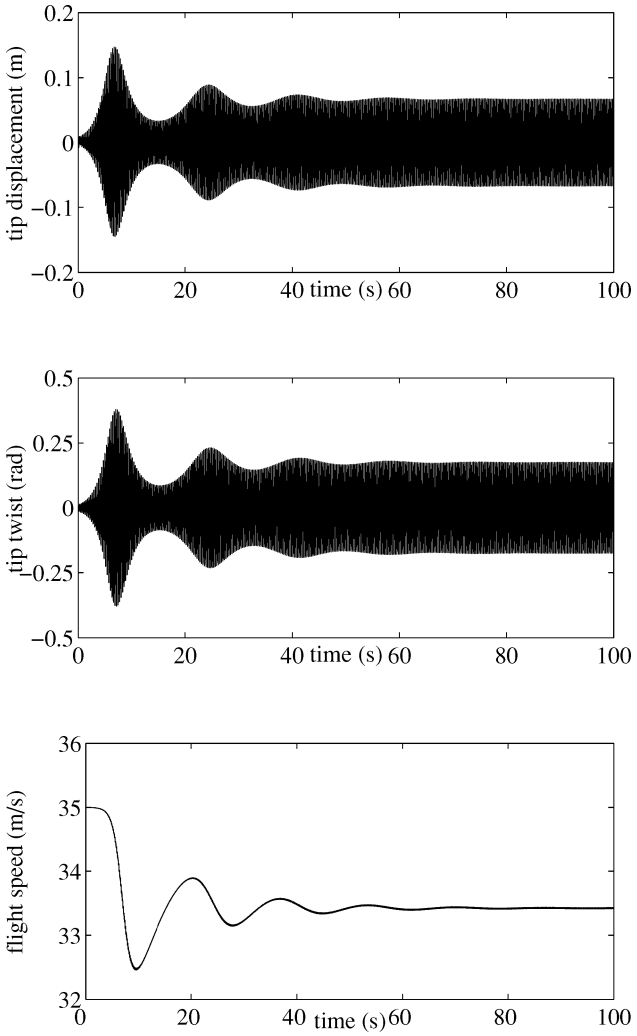

Fig. 5 Limit-cycle oscillations caused by flutter-induced drag at $U = 35$ m/s.

Now, for higher trim flight speeds the trim thrust required is higher. The difference between the trust provided and the thrust required (at the flutter speed) will be higher, and thus the LCO amplitude will be higher. Figures 6–8 show the LCO of the aircraft at various trim conditions. Figure 6 shows the time history of tip displacement at various trim thrust level, Fig. 7 shows the corresponding plots for tip twist, and Fig. 8 shows the corresponding plots for flight speed. It is seen that for flight speeds above the flutter speed the disturbance initially grows exponentially, and then the vibration amplitude and flight speed oscillate. For higher trim flight speed, the amplitude and frequency of oscillations in the vibration amplitude and the flight speed are higher. Also, as expected the converged, steady-state LCO vibration amplitude is higher for higher trim flight speed.

Figure 9 shows the plot of steady-state LCO amplitude (tip twist) as a function of trim flight speed. At steady state, the aircraft is at the flutter speed for all of the different trim flight speeds. In essence, the trim flight speed is an indication of the trim thrust. Higher trim flight speed indicates higher thrust from the engine. As the trim thrust is increased to that required for flight speeds above the flutter speed, there is LCO. The amplitude of LCO increases with the trim thrust.

Figures 10 and 11 show the effect of the drag coefficient and the fuselage mass on the LCO of the aircraft respectively. The plots show the response in terms of the flight speed. From Eq. (7) it is clear that if C_{D_0} increases or M_{aircraft} decreases the frequency of oscillation of flight speed will increase. The plots show such a change in the LCO with variation in C_{D_0} and M_{aircraft}. The plots also show that as the C_{D_0} decreases or M_{aircraft} increases it takes longer to reach the steady-state LCO.

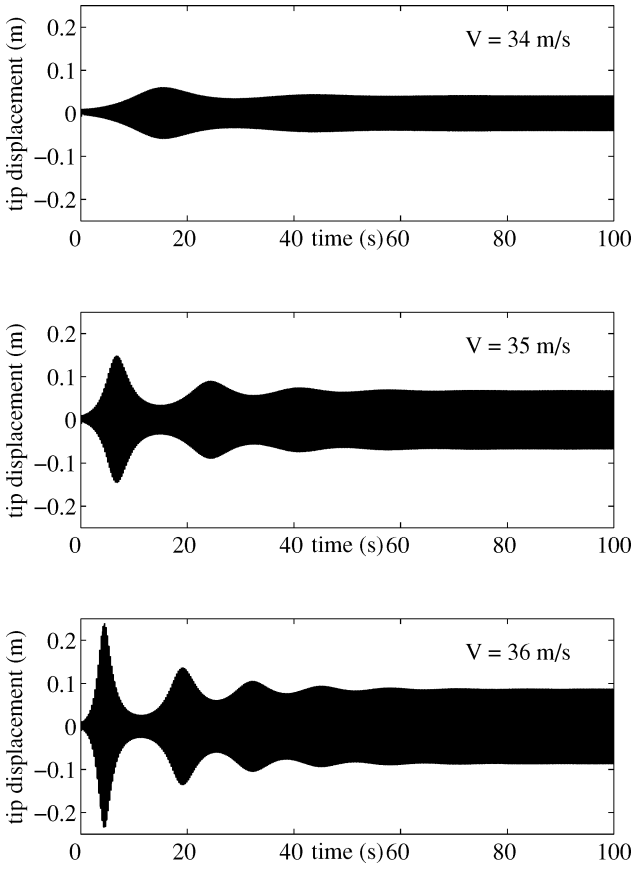

Fig. 6 LCOs at various trim flight speeds (tip displacement).

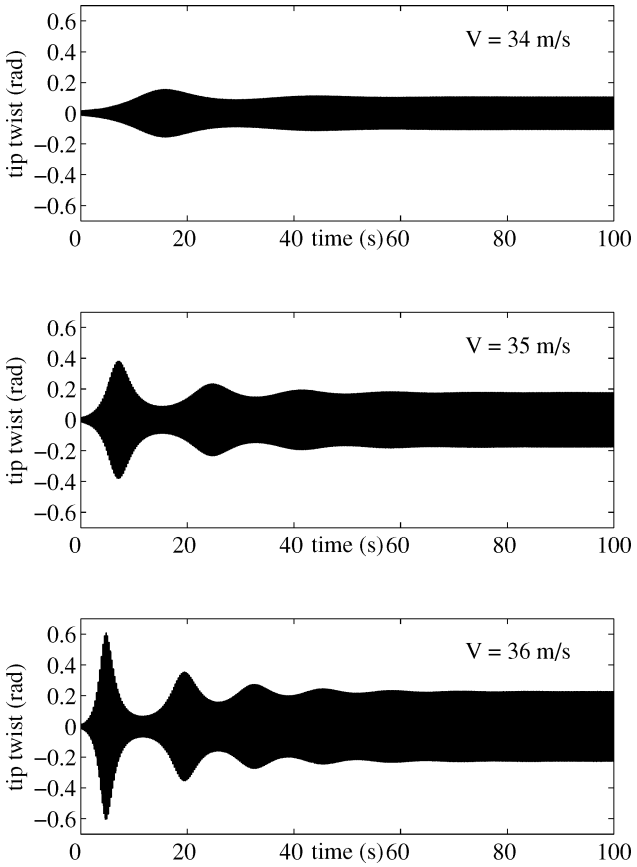

Fig. 7 LCOs at various trim flight speeds (tip twist).

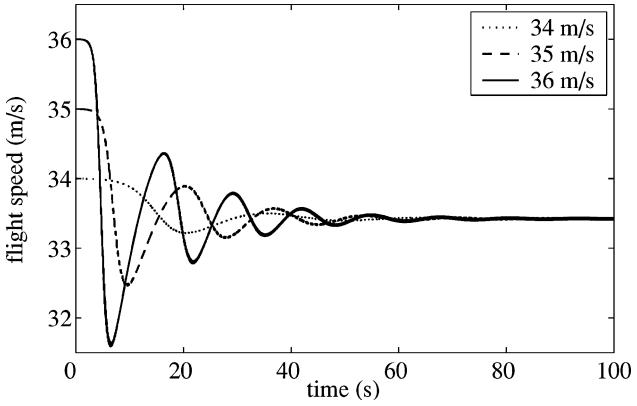

Fig. 8 LCOs at various trim flight speeds.

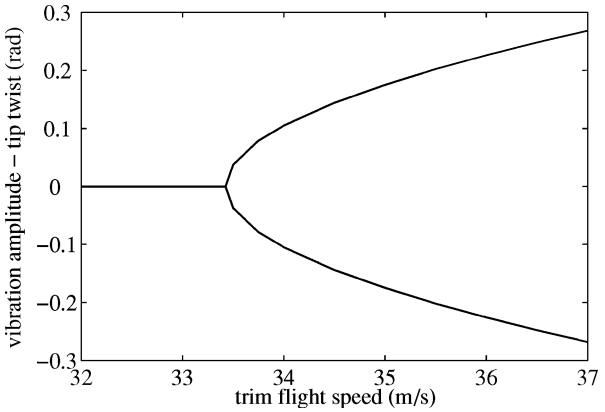

Fig. 9 LCO amplitude as a function of trim flight speed.

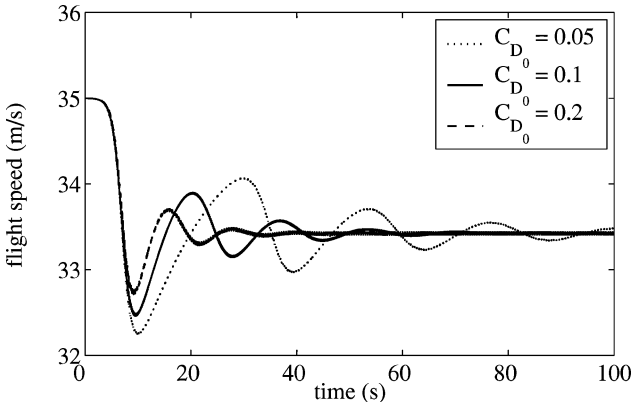

Fig. 10 Effect of drag coefficient on the LCO at $U = 35$ m/s.

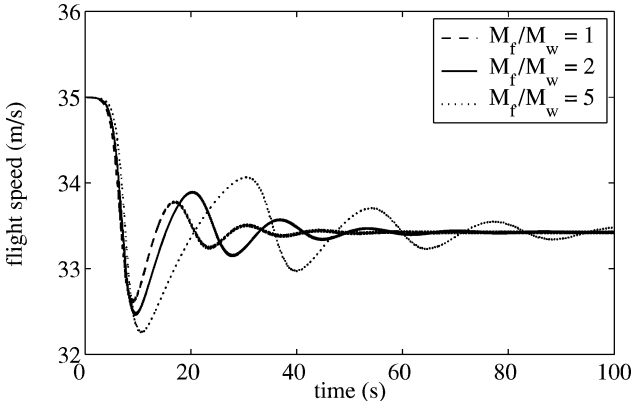

Fig. 11 Effect of aircraft weight on the LCO at $U = 35$ m/s.

Conclusions

The paper examines the limit-cycle-oscillation (LCO) behavior caused by the induced drag accompanying flutter vibrations. If the complete aircraft is considered, the induced drag couples the wing aeroelastic equations with the flight-speed equation. Thus, the vibration amplitude and flight speed are interdependent. When disturbed at a flight speed above the flutter speed, the flight speed as well as the amplitude of vibration oscillates initially. Eventually the vibrations converge to a steady, periodic, sinusoidal oscillation of the wing while the flight speed converges to the flutter speed. LCOs for various trim flight speeds, viscous drag coefficients, and aircraft weights are presented.

The present work does not take into account the nonlinear characteristics of the wing. Even for vibration response in the nonlinear range, the actual response of the aircraft can be completely described only if, in addition to nonlinear structural and aerodynamic model, flutter-induced drag is included in the analysis.

References

[1]Dunn, P., and Dugundji, J., "Nonlinear Stall Flutter and Divergence Analysis of Cantilevered Graphite/Epoxy Wings," *AIAA Journal*, Vol. 30, No. 1, 1992, pp. 153–162.

[2]Tang, D. M., and Dowell, E. H., "Experimental and Theoretical Study for Nonlinear Aeroelastic Behavior of a Flexible Rotor Blade," *AIAA Journal*, Vol. 31, No. 6, 1993, pp. 1133–1142.

[3]O'Neil, T., and Strganac, T. W., "Aeroelastic Response of a Rigid Wing Supported by Nonlinear Springs," *Journal of Aircraft*, Vol. 35, No. 4, 1998, pp. 616–622.

[4]Patil, M. J., Hodges, D. H., and Cesnik, C. E. S., "Limit Cycle Oscillations in High-Aspect-Ratio Wings," *Journal of Fluids and Structures*, Vol. 15, No. 1, 2001, pp. 107–132.

[5]Patil, M. J., "From Fluttering Wings to Flapping Flight: The Energy Connection," *Journal of Aircraft*, Vol. 40, No. 2, 2003, pp. 270–276.

[6]Hall, K. C., "Eigenanalysis of Unsteady Flows About Airfoils, Cascades, and Wings," *AIAA Journal*, Vol. 32, No. 12, 1994, pp. 2426–2432.

[7]Cicala, P., "Present State of Development in Nonsteady Motion of a Lifting Surface," NACA TM 1277, Oct. 1951; translated from *Aerotecnica*, 1941.